Clinical identification of malignant pleural effusions in the emergency department

Ioannis Psallidas[1,2,3], Antonia Marazioti[1], Apostolos Voulgaridis[4], Marianthi Iliopoulou[1], Anthi C. Krontira[1], Ioannis Lilis[1], Rachelle Asciak[3,5], Nikolaos I. Kanellakis[1,3], Argiro Papapavlou[6], Seferina Mavroudi[6,7], Aigli Korfiati[6], Konstantinos Theofilatos[6,8], Vassileios Tarnaris[1], Najib M. Rahman[3,5], Kyriakos Karkoulias[4], Konstantinos Spyropoulos[4], and Georgios T. Stathopoulos[1,9]

1 Laboratory for Molecular Respiratory Carcinogenesis, Department of Physiology, Faculty of Medicine; University of Patras; 1 Asklepiou Str., 26504, Rio, Achaia, Greece.

2 Lungs for Living Research Centre, UCL Respiratory, University College London, London, UK

3 Laboratory of Pleural and Lung Cancer Translational Research, Nuffield Department of Medicine, University of Oxford, Oxford, OX3 7FZ, UK

4 Department of Pulmonary Medicine, Rio University Hospital, Faculty of Medicine, University of Patras, 26504 Rio, Greece.

5 Oxford Centre for Respiratory Medicine, Churchill Hospital, Oxford University Hospitals NHS Foundation Trust, Oxford, OX3 7LE, UK.

6 Intelligent Systems Biology (InSyBio) Ltd., Innovations House, 19 Staple Gardens, Winchester, SO23 8SR and Patras Science Park building, 26504Platani, Patras, Greece.

7 Department of Social Work, School of Sciences of Health and Care, Technological Educational Institute of Western Greece, Megalou Alexandrou 1, Koukouli, 26334 Patra, Greece.

8 Department of Cardiovascular Research, Kings College, Strand, London WC2R 2LS, England, United Kingdom

9 Comprehensive Pneumology Center (CPC) and Institute for Lung Biology and Disease (iLBD), University Hospital, Ludwig-Maximilian University (LMU) and Helmholtz Center Munich, Member of the German Center for Lung Research (DZL); Max-Lebsche-Platz 31, 81377, Munich, Bavaria, Germany

*** Corresponding author:** Georgios T. Stathopoulos (gstathop@upatras.gr). Biomedical Sciences Research Building, 2nd floor, Room B40; 1 Asklepiou Str., University Campus, 26504 Rio, Greece; Phone: +30-2610-969154/116/170; Fax: +30-2610-969176.

Conflict of interest: I.P. works as a Senior Director in AstraZeneca Pharmaceutical in a non-related field with the publication. The remaining authors have declared that no conflict of interest exists.

Word count, manuscript: 3,902.

ABSTRACT

Background: Pleural effusions (PE) most commonly signal either pleural-disseminated infection or cancer. Simple and rapid diagnostic markers of pleural malignancy at patients' admission that streamline diagnostic, treatment, and research efforts remain unidentified. The objective of the study was to identify and validate predictors of malignancy of PE at admission.

Methods: A prospective cohort of 360 patients with PE from different etiologies was recruited between 2013 and 2017 (ClinicalTrials.Gov NCT03319472). Data collected within 4 hours of admission included history, chest X-ray, and blood/pleural fluid cell counts and biochemistry. Binary regression and receiver-operator analyses using malignancy as the target were used to develop the malignancy of pleural effusion in the emergency department (MAPED) score. MAPED was retrospectively validated in a separate cohort (n = 241).

Results: Five variables emerged from binary regression as independent predictors of malignant PE. Receiver-operator curves determined optimal cut-offs and repeat binary regression of thresholded variables identified hazard ratios for development of the weighted MAPED score. Age > 55 years and X-ray PE size > 50% of lung field (2 hazard points each), unilateral effusion, pleural fluid neutrophils < 10%, and PF protein > 3.5 g/dL (1 hazard point each) were used to compile MAPED (scoring 0-7 points), which yielded an area under curve of 0.824 ($P < 10^{-23}$) in the derivation cohort and 0.677 ($P = 2 \times 10^{-6}$) in the validation cohort.

Conclusion: MAPED can identify malignant PE within 4 hours of admission with 75% accuracy and can be a useful clinical and research tool.

Word count abstract: 249

Key words: malignant pleural effusion; cancer; age; emergency department; neutrophil; bilateral; protein.

INTRODUCTION

Pleural effusions (PE) are common conditions that annually affect an estimated 1.5 million individuals in the US alone (1). PE are caused by involvement of the pleural space by cancer (malignant PE, MPE), by microorganisms, by inflammatory processes, or by deranged Starling pressures along juxtapleural blood and lymphatic vessels, among other causes hereafter collectively referred to as benign PE (BPE) (1). Most patients with PE are hospitalized for diagnosis and treatment, a time-point when they face a tremendously dichotomous outcome: patients with MPE anticipate a median survival of a few months (2-4), while those with BPE fare significantly better (1). While the time and procedures required for placement of a definitive cell- or tissue-based diagnosis of MPE or an etiologic diagnosis of BPE are usually substantial, a simple model to predict malignancy that would rapidly inform physicians of the probability of cancer is missing.

To bridge this gap, we initiated a prospective study aimed at diagnosing malignancy of PE in the emergency department (MAPED; ClinicalTrials.Gov NCT03319472). For this, we prospectively evaluated 439 patients with PE that were admitted to our emergency wards between 2013 and 2017. We collected simple clinical, pleural fluid (PF) and blood (B), and chest X-ray data that were available within four hours after admission. The end-point was definitive diagnosis of MPE or BPE within a month, which was achieved in 360 patients. We employed multiple layers of analyses, including MPE-BPE comparisons, binary logistic regression, and receiver-operator curves (ROC), to identify variables that independently predict malignancy after a month and used this information to build the MAPED model. MAPED was 82% accurate in predicting cancer in PE in the derivation cohort and a slightly modified version was 68% accurate in a validation cohort of 241 patients with PE from Oxford, UK.

RESULTS

Clinical, radiologic, cytometric and biochemical differences between malignant and benign pleural effusions on admission

Out of the first 439 patients with PE prospectively enrolled into the MAPED study, a definitive diagnosis within 30 days was made in 360 patients (82%), underpinning the difficult and time-consuming management of this patient group (3). A schematic flowchart of the study is presented in Figure 1, a color-coded heatmap of the raw clinical data recorded from the 360 patients that met this primary end-point and were further analyzed is given in Figure 2, and a data summary in Table 1. One hundred two patients were diagnosed based on cytology and the remaining 43 required tissue-based diagnoses. Sixty four patients had lung cancer (44%), 32 breast cancer (22%), 22 malignant pleural mesothelioma (15%), 11 gynecological malignancies (8%), six gastrointestinal tumors (4%), five hematological malignancies (3%), and five other cancers (3%), proportions that were in accord with previous studies from the same geographic region (2, 4). Several differences were identified when patients with BPE and MPE were compared (Figure 3 and Table 1). Overall, MPE were more frequently unilateral and large in size compared with BPE (Figure 3A). In addition, patients with MPE had increased relative and/or absolute numbers of red blood cells and lymphocytes in PF, decreased relative and/or absolute numbers of nucleated cells and neutrophils in PF, more peripheral blood lymphocytes, as well as elevated levels of LDH and protein in PF compared with BPE (Figure 3B). These results indicated that there are significant differences between BPE and MPE at admission that can possibly be exploited to estimate the risk of malignancy.

Independent predictors of malignancy of pleural effusion at admission

In order to identify variables that predict underlying cancer, all variables recorded were entered into ROC analyses, which identified 12 variables [age, PE size, PF/B nucleated cell count ratio, PF neutrophils (percentage and count), PF lymphocytes (percentage), PF/B neutrophil ratio (ratio of percentages and counts), PF/B lymphocyte ratio (ratio of percentages), PF LDH levels, and PF/serum LDH and protein ratios] as inputs significantly associated with incipient diagnosis of MPE and set their optimal cut-offs (Figures 4A, 4B). Interestingly, the last three variables represent Light's criteria used to distinguish exudates from transudates; however, our ROC analyses identified optimal cut-offs that differed from those used by Light (5). Subsequently, raw variables that emerged from either direct MPE-BPE comparisons (n = 19) or from ROC (n = 12) were entered into binary logistic regression analyses using malignancy as target. Of the n = 20 variables entered, five were identified as independent predictors of MPE: age, PE size, PF neutrophil percentage and protein levels, as well as PE laterality (Figure 4C). These were thresholded according to ROC-defined optimal cut-offs and were re-entered into ROC using MPE as target. Indeed, thresholded variables retained their linkage with the outcome measure and their independent predictive power of malignancy in repeat binary logistic regression analyses that were used to generate risk estimates (Figures 4D–4F).

A tool to predict malignancy of a pleural effusion at admission (MAPED)

The relative risk ratios from binary logistic regression were incorporated into a simple weighted MPE risk score named MAPED after the present study (Figure 5A). MAPED was calculated for all 360 patients in the discovery dataset, assigning two risk points each to patients aged > 55 years or with effusions occupying > 50% of the lung field, and one risk point each to patients with PF neutrophils < 10%, PF protein > 3.5 g/dL, or a unilateral effusion (Table 2). MAPED scores were significantly differently distributed in patients with

BPE and MPE (Figure 5B), and could identify MPE with 82% accuracy in the derivation cohort (Figures 6A–6D). MAPED performed reasonably well in the prediction of a malignant cytology result, but even better in predicting the final diagnosis (Figures 6E–6G). Since Light's criteria, an established means to classify exudative from transudative PE with the former class of PE encompassing most MPE, also emerged from our ROC analyses but did not withstand regression, we next sought to compare MAPED (developed to predict cancer in PE) with classical Light's criteria (developed to predict exudative PE) as well as Light's criteria with cut-offs optimized for MPE prediction by our ROC analyses (PF LDH > 250 U/L, PF/serum LDH ratio > 0.9, and PF/serum protein ratio > 0.6; Figure 4B). MAPED and Light's criteria were unrelated and performed differently in the discovery cohort, while MAPED was more closely linked to a malignant diagnosis than both classical and modified Light's criteria (Figure 7).

External MAPED validation

We finally sought to determine the accuracy of MAPED in discriminating MPE from BPE in a separate cohort. We chose the Oxford Radcliffe Pleural Biobank (ORPB), because this is one of the few cohorts where pleural effusion size was determined and where PF neutrophil data are also available, although in a different format compared with MAPED (neutrophil versus lymphocyte predominance as compared with our quantitative cellular data). Despite these discrepancies, MAPED performed reasonably well in 241 (128 with BPE and 113 with MPE) patients from ORPB, correctly predicting MPE from admission data in 68% of patients (Figures 8A–8C). Two-way ANOVA of MPE probabilities when patients were stratified by MAPED score in the discovery and validation datasets combined showed that MAPED score significantly impacted MPE likelihood irrespective of study site (Figure 8D). We finally set out to compare MAPED with computer-assisted classification of our patients with PE. For

this, all available raw data were entered into ConsensusCluster, academic software designed for unsupervised clustering of numerical data (6). ConsensusCluster identified two bigger and another four small groups of patients in the MAPED cohort without any guidance (Figure 9A). Binary logistic regression analyses using raw variables as inputs and ConsensusClusters as targets revealed that PE size and protein content were the variables that heavily defined the two big clusters. However, ConsensusClusters were not correlated with PE diagnosis, while MAPED was (Figure 9B). These results suggest that our supervised analyses tailored to devise MAPED according to the variable that matters (BPE versus MPE) cannot be substituted by unsupervised computer-assisted analyses. Interestingly, the software came up with PE size and PF protein content as the defining features of PE, both identified as independent predictors of malignancy of PE in the present study.

Retrospective follow-up of MAPED patients

Two years after the conclusion of the MAPED study, all patients were retrospectively revisited to identify possible ill-classification of occult MPE as BPE at the 30-day time-point. This included review of hospital patient charts in 255 patients, outpatient visits in 82 patients and both in 23 patients. All patients initially diagnosed with MPE were confirmed to have malignant disease at follow up, while only five patients with initial diagnoses of BPE were found to have MPE during follow up (1.4% misclassification rate): three had malignant pleural mesothelioma, one had lung cancer-associated MPE, and yet another had lymphoma. We have no way of knowing whether these patients had cancer initially or developed cancer after MAPED conclusion. However, even when these five patients were classified as having MPE instead of BPE, MAPED retained its diagnostic accuracy in the MAPED cohort (AUC = 0.815; $P = 10^{-25}$).

DISCUSSION

The present study attempts to address a clinically challenging problem: to determine the likelihood of malignancy of a pleural effusion on patient admission to the emergency department using simple clinical and bedside test parameters that are available at admission throughout the world. The study analyzed 360 patients with a definitive PE diagnosis, which was met by 82% of enrolled patients over four years. MAPED showed that multiple parameters can distinguish MPE from BPE. Moreover, five variables combined into the MAPED score can prospectively predict malignancy of a PE in 68-82% of cases in both the derivation and the external validation cohorts.

The accuracy of MAPED is satisfactory given its simplicity. Another effort to build a score similar to MAPED was limited by retrospective design, inclusion of patients with uncertain diagnoses, multiple primary end-points, and lack of external validation (7). A chest computed tomography (CT)-based score derived from 343 prospectively enrolled patients with PE achieved area under curve (AUC) of 0.919 in discriminating MPE from BPE (8). However, contrast-enhancement and scan reading by two blinded radiologists with > 20 years' experience was required, increasing risk, cost, and time. Despite the careful design and the prospective nature of the study, interobserver agreement was only 0.55–0.94. To scan our 360 discovery and 241 validation patients assuming a cost of € 200/scan and 0.5 hour physician time required for scan interpretation would cost € 120,200 and 300.5 radiologist hours. We used simple bedside tests done routinely during admission of a patient with PE to build MAPED, which performs only slightly inferior to the above-referenced CT score, at zero additional cost and physician time spent.

The predictors of malignancy identified here are also worth mentioning. Aging is known to be linked with increasing risk of cancer (9), but its value in prospectively differentiating MPE

from BPE has never been identified and exploited, as most studies did not detect age differences between patients with MPE and BPE (1, 2, 4, 10). We did, and although the mean age difference between our patients with BPE and MPE was small (seven years), an age cut-off of 55 years alone could discriminate MPE from BPE with AUC of 0.617. This was not the case in the ORPB validation set, where an age cut-off of 55 years produced an AUC of 0.513 ($P = 0.722$). Notwithstanding population and healthcare accessibility differences between Greece and the UK that can explain this discrepancy (https://knoema.com/;accessed 31.10.2017) and may necessitate different age cut-offs in different countries, we chose to develop a generally applicable MAPED score and applied it to ORPB patients.

Relative neutrophil predominance in pleural fluid is also a well-known hallmark of infectious BPE due to common pathogens (3, 5), but has never been used as a negative marker of PE malignancy. Interestingly, one of the most important studies in the field identified blood neutrophil-to-lymphocyte count ratio as an important determinant of the survival of patients with MPE (2). However, the use of relative pleural neutrophil abundance to rule out MPE is hampered by the common practice of not accurately counting cells in PF by most hospitals in the US and Europe. We overcame this by establishing PF differential counts as routine practice in our hospital for the purposes of MAPED. The effort was well worth it, since neutrophil percentage < 10% produced an AUC of 0.609 in MAPED. Again, this was not the case in ORPB, where PF neutrophil paucity produced an AUC of 0.535 ($P = 0.352$). However, neutrophil paucity in ORPB was defined as neutrophil percentage < 50% and not < 10% as in MAPED.

Unilaterality of PE was also an indicator of possible malignancy in our hands, since 97% of MPE but only 88% of BPE were unilateral. This was not evident in the ORPB study, where 90% of BPE and 91% of MPE were unilateral ($P = 0.730$; χ^2test). As the numbers of

unilateral BPE largely agree for both cohorts, we postulate that more MPE were classified as bilateral in the ORPB study due to the higher sensitivity for diagnosing a PE in this pleural referral center. Interestingly, 70% of BPE and 79% of MPE in an above-referenced CT study were unilateral, failing statistical significance by a margin ($P = 0.080$; χ^2test) (8). The different proportions observed in PE laterality between MAPED and the above study are likely attributable to the high sensitivity of chest CT in detecting PE as compared with chest X-ray.

Unlike the aforementioned predictors of MPE that failed to perform well in the ORPB validation cohort, PE size > 50% of the lung field and PF protein levels > 3.5 g/dL did perform excellently in both MAPED and ORPB. In specific, only 27% of BPE but an astonishing 58% of MPE fulfilled the size criterion in ORPB ($P = 10^{-5}$; χ^2test) compared with 5% and 46% in MAPED, respectively, with higher numbers for ORPB BPE likely attributable to a higher prevalence of heart failure. In addition, 59% of BPE and 78% of MPE fulfilled the protein criterion in ORPB ($P = 10^{-3}$; χ^2test) compared with 68% and 88% in MAPED, respectively ($P = 3 \times 10^{-5}$; χ^2test), with the similar results probably owing to more uniform methods of measurement, since pleural fluid/blood protein ratio is an established Light's criterion (3, 5). Size and protein criteria also produced significant AUC values in ORPB, comparable to MAPED counterparts: 0.655 ($P = 3 \times 10^{-5}$) and 0.596 ($P = 0.010$). Although it is well established that MPE pathogenesis includes increased vascular permeability leading to protein-rich exudate (11), pleural fluid-to-blood protein ratio is an exudate criterion according to Light (3, 5), and protein measurements are routine in contemporary hospitals, PF protein levels have never been exploited to diagnose malignancy of MPE. To this end, pleural fluid LDH levels > 1500 U/L were recently proposed as a poor prognosis marker for MPE (2), and high MPE protein levels were found in a previous study (8), rendering our findings plausible. Massive PE have rarely been studied separately,

although they are common with both BPE and MPE (12, 13). In the largest study looking at PE size, Porcel et al. classified 535 patients with BPE and 231 with MPE into three size categories based on posterior-anterior chest X-rays: non-large PE was defined as occupying less than two thirds of the lung field, large as occupying more than that, and massive as occupying the whole lung field (12). Interestingly and in accord with our results, the authors found that 24% of non-large, 49% of large, and 59% of massive PE were malignant ($P < 10^{-5}$; χ^2 test), but this pearl has never been used to estimate the risk for PE malignancy.

The present study has limitations. First, the general applicability of MAPED may be hampered by population, measurement, and practice differences between countries, as well as by divergent prevalence of specific causes of PE. However, MAPED withstood testing in such a suboptimal setting. In addition, the relative prevalence of MPE in MAPED (40% of all PE) was similar to most other published studies from Europe and North America that report values from 30–54% (1, 6, 12). A second potential limitation is chest X-ray interpretation, the only non-standardized measure included in the MAPED score. However, judging whether a PE occupies more or less of half of a lung field is task easily tackled even by non-specialist physicians, as opposed to complex CT scoring. Third, due to its design, MAPED cannot be used in outpatients, as well as in patients with previous PE or cancer. Finally, the short follow-up (one month) permitted in MAPED for the definitive diagnosis means that there will be some patient misclassification, since some MPE are diagnosed after years from the first appearance of PE (14). However, this study design was chosen because an acute diagnosis of cancer in the clinical setting of a PE was the main question behind MAPED.

In conclusion, the simple MAPED score is shown to predict the presence of malignancy of a pleural effusion at admission in 75% of the cases examined in two countries, at no additional risk to patients, cost to healthcare systems, and time spent to caring physicians. Pending

further validation, MAPED is positioned to contribute to improvements in patient management and research design, since it alters the likelihood of malignant disease at admission as a rule out or rule in score.

METHODS

MAPED study: MAPED was conducted in accord with the Declaration of Helsinki, reported in accord to the Transparent Reporting of Evaluations with Nonrandomized Designs (TREND) (15), was registered with ClinicalTrials.gov (NCT03319472; https://clinicaltrials.gov/ct2/show/NCT03319472?term=NCT03319472&rank=1),and written informed consent was obtained from all patients *a priori*. All patients with a chest X-ray-based PE diagnosis admitted to the emergency wards of the General Regional University Hospital of Patras, Greece, between 21/11/2013–21/11/2017 were prospectively evaluated for enrollment. Inclusion criteria were new diagnosis of PE and age > 18 years, while exclusion criteria were immediate discharge from the emergency department, previous pleural disease, and known cancer. Inpatients were chosen, since it was deemed that the percentage of patients that would meet the primary end-point would be higher and patient loss to follow-up would be smaller compared with outpatients. Baseline data prospectively obtained within four hours after admission were derived from routine diagnostic testing including history, chest X-ray, blood counts and biochemistry, and pleural fluid (PF) pH, cell counts, and biochemistry. Recorded variables were: age (years); smoking status (never, former, or current); PE side (right, left, or bilateral); PE size score (% of lung field occupied on chest X-ray: 1, <10%; 2, 11-25%; 3, 26-50%; 4, 51-75%;and 5, >75%; the larger of two descriptors was used for bilateral PE); Pleural Fluid (PF) and blood red blood cells (/μl); PF nucleated and blood white blood cells (/μl); PF and blood differential nucleated cell counts (% mononuclear, neutrophil, lymphocytic, and eosinophil cells); PF and serum lactate dehydrogenase (LDH; U/L), protein (g/dL), glucose (mg/dL); and PF pH. Values calculated from these primary data were: PF and blood absolute nucleated cell counts (mononuclear, neutrophil, lymphocytic, and eosinophil cells /μl); PF/blood red, nucleated, mononuclear, neutrophil, lymphocytic, and eosinophil cell ratios; and PF/serum LDH, protein, and glucose

ratios. Light's criteria were calculated for each patient. The end-point of the study was a definitive etiologic PE diagnosis within 30 days after admission. MPE was diagnosed exclusively based on identification of malignant cells and/or tissues in pleural samples. BPE was diagnosed using a constellation of criteria diagnostic of infection (positive pleural fluid smears, cultures, or polymerase chain reaction for common pathogens or Mycobacteria; lymphocytic-predominant exudative effusion with recent tuberculin skin test conversion or conversion within a month after admission; full remission of PE and lung lesions on empiric antibacterial or antituberculous treatment within a month after admission; or caseating granulomas in pleural tissue), heart failure (transthoracic echocardiography-determined ejection fraction < 40% with/without tricuspid regurgitation and/or diastolic dysfunction and/or elevated serum N-terminal pro-B-type natriuretic peptide levels), or other diseases (hypoproteinemia, ascites, post coronary artery by-pass grafting, etc.), according to current practice guidelines (1, 3). Results from all patients were assessed by a multidisciplinary team 30 days post-admission to confirm a definitive diagnosis, the primary end-point. The same team retrospectively revisited all patients two years after the conclusion of the MAPED study, in order to identify possible ill-classification of occult MPE as BPE. For this, hospital patient charts were reviewed in 255 patients, outpatient visits of 82 patients were performed, and both were done for another 23 patients.

Oxford validation cohort: Subjects from the Oxford Radcliffe Pleural Biobank (ORPB) were used for external validation of MAPED. In total, 241 patients (128 with BPE and 113 with MPE) were included in the validation cohort. The variables extracted from ORPB records were: age (years); PE side (unilateral or bilateral); PE size score (% of lung field occupied on chest X-ray or computed tomography: 0, ≤ 50%; 1, > 50%); PF neutrophil predominance (yes or no); and PF protein (g/dL) and were used to calculate a modified MAPED score.

Statistics: Minimal study size (n^{MIN}) was determined by two lines of power analyses (http://www.gpower.hhu.de/en.html): employing Fischer's exact test to assess proportion inequalities between two independent groups, α error = 0.05, 80% power, and 1:1 allocation ratio, n^{MIN} = 314 was required to detect the difference between 0% and 5% and n^{MIN} = 348 between 30% and 45%; employing Student's t-test to detect differences in means between two independent groups, αerror = 0.05, 90% power, effect size d = 0.3, and 1:1 allocation ratio, n^{MIN} = 382 was required. We targeted recruitment to n = 360, which was achieved in 11/2017. There were no missing data for the outcome measure. Among the predictors, missing data ranged from 0-29% and no data were imputed. Data distribution was tested using Kolmogorov-Smirnov test. Data summaries are given as frequencies or point estimates (mean or median) with descriptors of dispersion (standard deviation, SD or interquartile range, IQR or 95% confidence interval, 95%CI) as appropriate and indicated. Differences between variables in BPE versus MPE groups were examined using Fischer's exact or Mann-Whitney U-tests, depending on variable nature, as appropriate and as indicated. Probability (P) values < 0.05 were considered significant. Receiver-operator curves (ROC) of raw variables as inputs and MPE as target were used to determine variables significantly associated with malignancy of PE and their optimal cut-offs. Binary logistic regression using backward Waldman elimination of raw variables as inputs and MPE as target was employed to identify independent predictors of malignancy of PE among variables that emerged from BPE-MPE comparisons or from ROC analyses. Repeat ROC of thresholded independent predictors as inputs and MPE as target were used to validate optimal cut-offs. Repeat binary logistic regression using backward Waldman elimination and thresholded independent predictors as inputs and MPE as target was employed to determine hazard ratios and to build the MAPED model. Unsupervised clustering was done using ConsensusCluster (6) that is freely available at: https://code.google.com/archive/p/consensus-cluster/. Settings were K=2-

6, subsample size = 300 and fraction = 0.8, K-means algorithm with single and average linkages, hierarchical consensus, and Euclidean distance metric, and scale principal component analysis normalization with fraction = 0.85 and Eigenvalue weight = 0.25. Analyses were done on the Statistical Package for the Social Sciences v24.0 (IBM, Armonk, NY) and Prism v8.0 (GraphPad, San Diego, USA).

Study approval

MAPED was approved by the University of Patras Ethics Committee (approval #22699/21.11.2013) and ethical and regulatory approval for the validation study was obtained by the South Central Oxford A Research Ethics Committee (REC reference number 15/SC/0186).

AUTHOR CONTRIBUTIONS

AM, AV, MI, ACK, IL, KK, and KS established and produced the clinical dataset from the Patras cohort; RA, NIK, NMR, and IP established and produced the clinical dataset from the Oxford cohort; AP, SM, AK, ACK, IL, KT, and VT performed data analyses; IP and GTS conceived the main idea and steered the study, developed the MAPED score, performed data analyses, and wrote the paper.

ACKNOWLEDGEMENTS

The authors thank the participant patients and the funders of this study, which was supported by European Research Council 2010 Starting Independent Investigator and 2015 Proof-of-Concept Grants (260524 and 679345, respectively, to GTS).

REFERENCES

1. Walker SP, et al. Nonmalignant Pleural Effusions: A Prospective Study of 356 Consecutive Unselected Patients. *Chest* 2017;151(5):1099–1105.

2. Clive AO, et al. Predicting survival in malignant pleural effusion: development and validation of the LENT prognostic score. *Thorax* 2014;69(12):1098–1104.

3. Light RW. Clinical practice. Pleural effusion. *N Engl J Med.* 2002;346(25):1971–1977.

4. Psallidas I, et al. Development and validation of response markers to predict survival and pleurodesis success in patients with malignant pleural effusion (PROMISE): a multicohort analysis. *Lancet Oncol.* 2018;19(7):930–939.

5. Light RW, Macgregor MI, Luchsinger PC, Ball WC Jr. Pleural effusions: the diagnostic separation of transudates and exudates. *Ann Intern Med.* 1972;77(4):507–513.

6. Seiler M, Huang CC, Szalma S, Bhanot G. ConsensusCluster: a software tool for unsupervised cluster discovery in numerical data. *OMICS* 2010;14(1):109–113.

7. Porcel JM, Vives M. Differentiating tuberculous from malignant pleural effusions: a scoring model. *Med Sci Monit.* 2003;9(5):CR175–180.

8. Porcel JM, Pardina M, Bielsa S, González A, Light RW. Derivation and Validation of a CT Scan Scoring System for Discriminating Malignant From Benign Pleural Effusions. *Chest* 2015;147(2):513–519.

9. Lozano R, et al. Global and regional mortality from 235 causes of death for 20 age groups in 1990 and 2010: a systematic analysis for the Global Burden of Disease Study 2010. *Lancet* 2012;380(9859):2095–2128.

10. Taghizadeh N, Fortin M, Tremblay A. US Hospitalizations for Malignant Pleural Effusions. Data From the 2012 National Inpatient Sample. *Chest* 2017;151(4):845–854.

11. Stathopoulos GT, Kalomenidis I. Malignant pleural effusion: tumor-host interactions unleashed. *Am J Respir Crit Care Med.* 2012;186(6):487–492.

12. Porcel JM, Vives M. Etiology and pleural fluid characteristics of large and massive effusions. *Chest* 2003;124(3):978–983.

13. Ryu JS, et al. Prognostic impact of minimal pleural effusion in non-small-cell lung cancer. *J Clin Oncol.* 2014;32(9):960–967.

14. Koegelenberg CF, Irusen EM, von Groote-Bidlingmaier F, Bruwer JW, Batubara EM, Diacon AH. The utility of ultrasound-guided thoracentesis and pleural biopsy in undiagnosed pleural exudates. *Thorax* 2015;70(10):995–997.

15. Des Jarlais DC, Lyles C, Crepaz N; TREND Group. Improving the reporting quality of nonrandomized evaluations of behavioral and public health interventions: the TREND statement. *Am J Public Health.* 2004;94(3):361–366.

FIGURE LEGENDS

Figure 1. Overview and flowchart of the malignancy of pleural effusion in the emergency department (MAPED) study (ClinicalTrials.Gov NCT03319472).

Figure 1

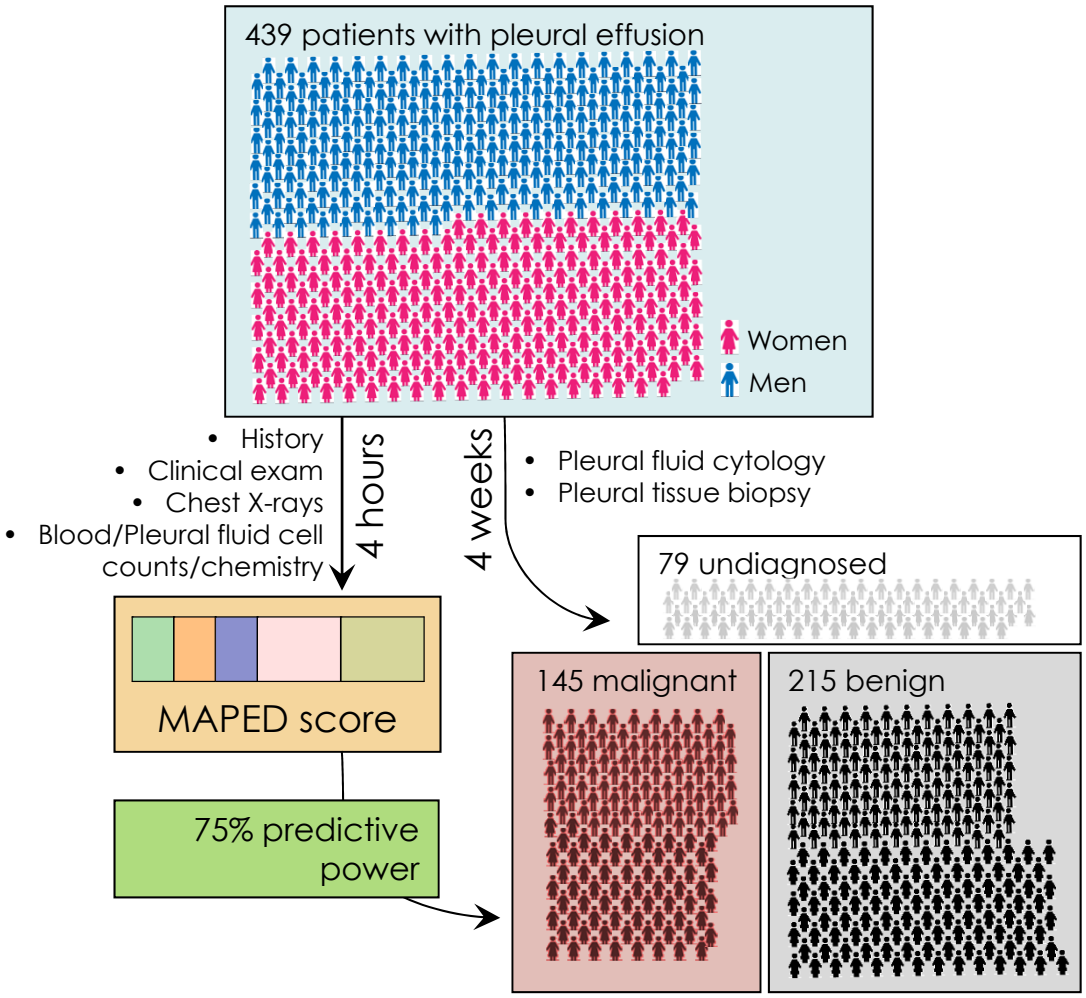
439 patients with pleural effusion
Women
Men
• History
• Clinical exam
• Chest X-rays
• Blood/Pleural fluid cell counts/chemistry
4 hours
4 weeks
• Pleural fluid cytology
• Pleural tissue biopsy
79 undiagnosed
MAPED score
75% predictive power
145 malignant
215 benign

Figure 2. Heatmap of raw data obtained from the malignancy of pleural effusion in the emergency department (MAPED) study. *n*, sample size; ID, identification number; PE, pleural effusion; PF, pleural fluid; WBC, white blood cells; NC, nucleated cells; B, blood; LDH, lactate dehydrogenase.

Figure 2

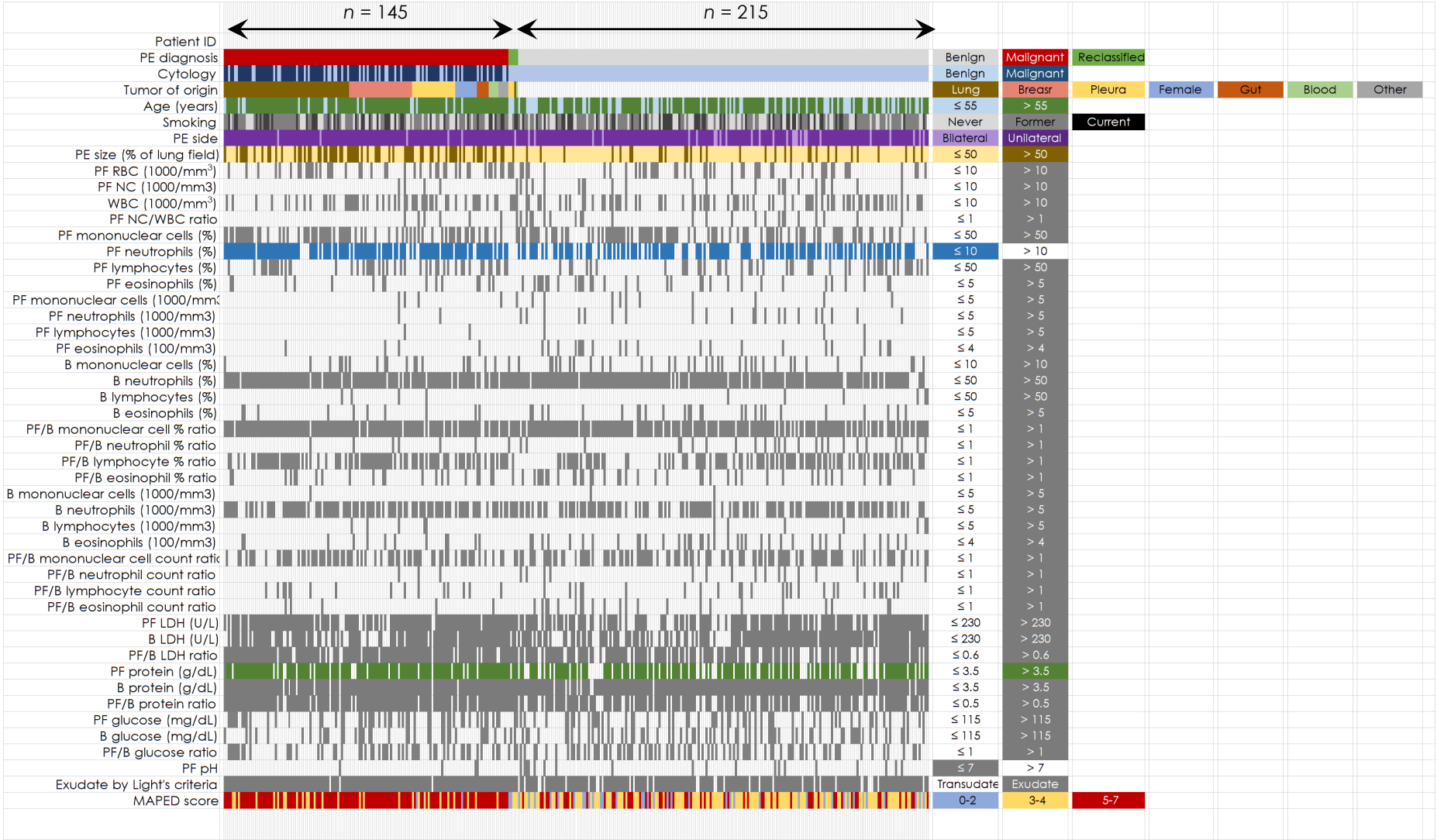
n = 145
n = 215
Patient ID
PE diagnosis
Cytology
Tumor of origin
Age (years)
Smoking
PE side
PE size (% of lung field)
PF RBC (1000/mm3)
PF NC (1000/mm3)
WBC (1000/mm3)
PF NC/WBC ratio
PF mononuclear cells (%)
PF neutrophils (%)
PF lymphocytes (%)
PF eosinophils (%)
PF mononuclear cells (1000/mm3
PF neutrophils (1000/mm3)
PF lymphocytes (1000/mm3)
PF eosinophils (100/mm3)
B mononuclear cells (%)
B neutrophils (%)
B lymphocytes (%)
B eosinophils (%)
PF/B mononuclear cell % ratio
PF/B neutrophil % ratio
PF/B lymphocyte % ratio
PF/B eosinophil % ratio
B mononuclear cells (1000/mm3)
B neutrophils (1000/mm3)
B lymphocytes (1000/mm3)
B eosinophils (100/mm3)
PF/B mononuclear cell count ratio
PF/B neutrophil count ratio
PF/B lymphocyte count ratio
PF/B eosinophil count ratio
PF LDH (U/L)
B LDH (U/L)
PF/B LDH ratio
PF protein (g/dL)
B protein (g/dL)
PF/B protein ratio
PF glucose (mg/dL)
B glucose (mg/dL)
PF/B glucose ratio
PF pH
Exudate by Light's criteria
MAPED score
Benign
Malignant
Reclassified
Benign
Malignant
Lung
Breast
Pleura
Female
Gut
Blood
Other
≤ 55
> 55
Never
Former
Current
Bilateral
Unilateral
≤ 50
> 50
≤ 10
> 10
≤ 10
> 10
≤ 10
> 10
≤ 1
> 1
≤ 50
> 50
≤ 10
> 10
≤ 50
> 50
≤ 5
> 5
≤ 5
> 5
≤ 5
> 5
≤ 5
> 5
≤ 4
> 4
≤ 10
> 10
≤ 50
> 50
≤ 50
> 50
≤ 5
> 5
≤ 1
> 1
≤ 1
> 1
≤ 1
> 1
≤ 1
> 1
≤ 5
> 5
≤ 5
> 5
≤ 5
> 5
≤ 4
> 4
≤ 1
> 1
≤ 1
> 1
≤ 1
> 1
≤ 1
> 1
≤ 230
> 230
≤ 230
> 230
≤ 0.6
> 0.6
≤ 3.5
> 3.5
≤ 3.5
> 3.5
≤ 0.5
> 0.5
≤ 115
> 115
≤ 115
> 115
≤ 1
> 1
≤ 7
> 7
Transudate
Exudate
0-2
3-4
5-7

Figure 3.Variables significantly different between benign (BPE) and malignant (MPE) pleural effusions (PE) in the MAPED study. (A) Frequency distributions of PE laterality and size by PE diagnosis. Shown are patient numbers (*n*) with Fischer's exact probabilities (*P*). **(B)** Continuous numerical variables stratified by diagnosis. Shown are kernel density distributions (violin plots), median and quartiles (lines), and Mann Whitney test probabilities (*P*). *n*, sample size; PF, pleural fluid; RBC, red blood cells; NCC, nucleated cell counts; B, blood; NΦ, neutrophils; LΦ, lymphocytes; LDH, lactate dehydrogenase.

Figure 3

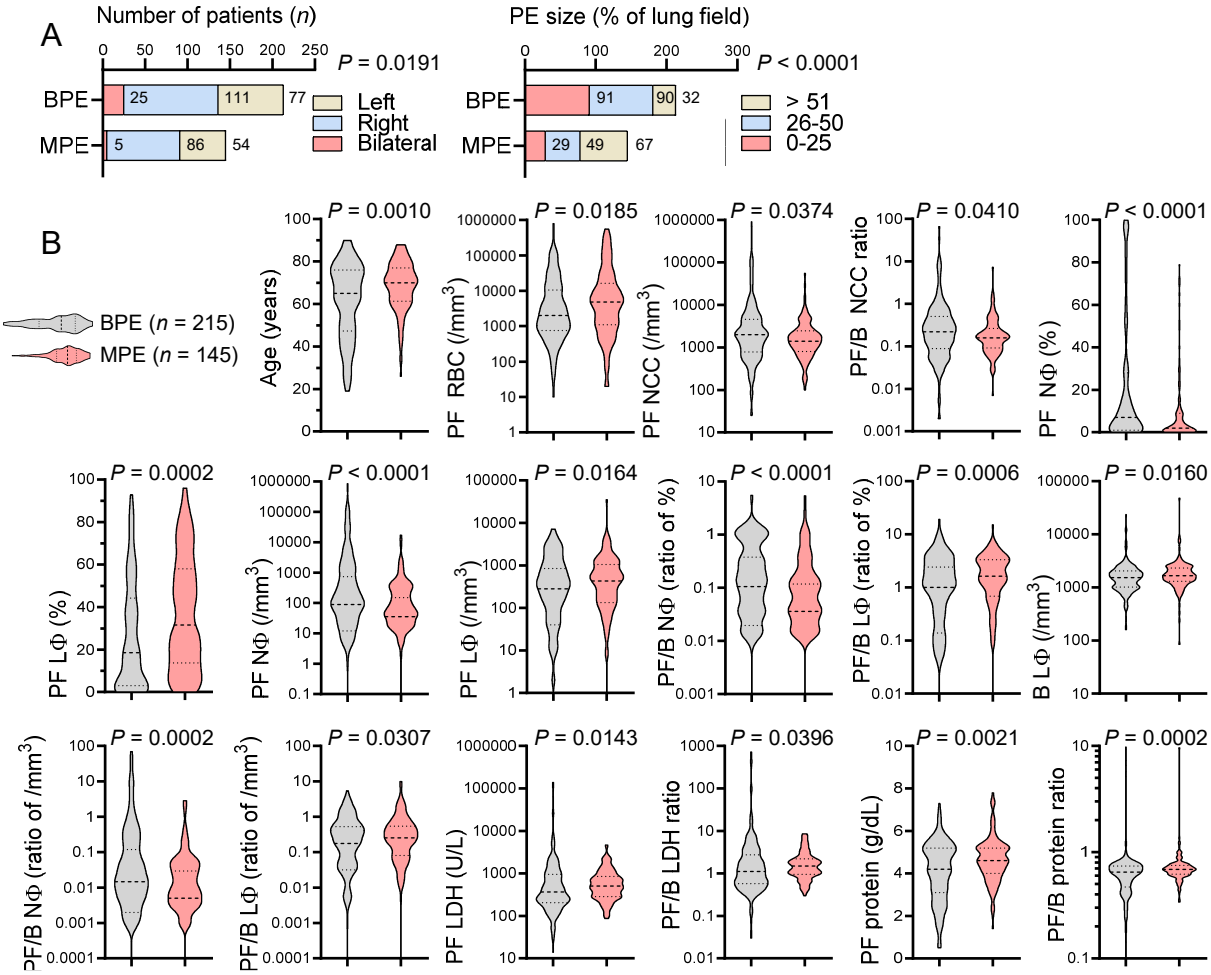
A
Number of patients (n)
0 50 100 150 200 250
P = 0.0191
BPE
MPE
25
111
77
5
86
54
Left
Right
Bilateral
PE size (% of lung field)
0 100 200 300
P < 0.0001
91
90
32
29
49
67
> 51
26-50
0-25
B
BPE (n = 215)
MPE (n = 145)
Age (years)
P = 0.0010
PF RBC (/mm3)
P = 0.0185
PF NCC (/mm3)
P = 0.0374
PF/B NCC ratio
P = 0.0410
PF NΦ (%)
P < 0.0001
PF LΦ (%)
P = 0.0002
PF NΦ (/mm3)
P < 0.0001
PF LΦ (/mm3)
P = 0.0164
PF/B NΦ (ratio of %)
P < 0.0001
PF/B LΦ (ratio of %)
P = 0.0006
B LΦ (/mm3)
P = 0.0160
PF/B NΦ (ratio of /mm3)
P = 0.0002
PF/B LΦ (ratio of /mm3)
P = 0.0307
PF LDH (U/L)
P = 0.0143
PF/B LDH ratio
P = 0.0396
PF protein (g/dL)
P = 0.0021
PF/B protein ratio
P = 0.0002

Figure 4. Development of a clinical tool to predict the malignancy of a pleural effusion in the emergency department. (A,B) Results of receiver-operator curve (ROC) analysis using raw variables as input and MPE as target showing curves (A) and tabular results (B) of areas under curve (AUC) with 95% confidence intervals (95%CI), probabilities (*P*), and optimal cut-offs. Grey shaded fonts indicate Light's criteria for differentiation between transudates and exudates (5). **(C)** Results of binary logistic regression using raw variables as input and MPE as target showing probability values (*P*) and proportional risk ratios (RR) with their 95% CI of the five independent predictors of MPE. **(D, E)** Results of ROC analysis using thresholded variables as input and MPE as target showing curves (D) and tabular results (E) of AUC with 95% CI and probabilities (*P*). **(F)** Results of binary logistic regression using thresholded variables as input and MPE as target showing probability values (*P*), proportional risk ratios (RR) with their 95% CI, and the MAPED risk points for each of the five independent predictors of MPE used to build the MAPED score. *n*, sample size; PE, pleural effusion; BPE, benign PE; MPE, malignant PE; PF, pleural fluid; RBC, red blood cells; NCC, nucleated cell counts; WBC, white blood cell counts; B, blood; NΦ, neutrophil; LΦ, lymphocyte; LDH, lactate dehydrogenase; LF, lung field; MAPED, malignancy of pleural effusion determined in the emergency department score.

Figure 4

A

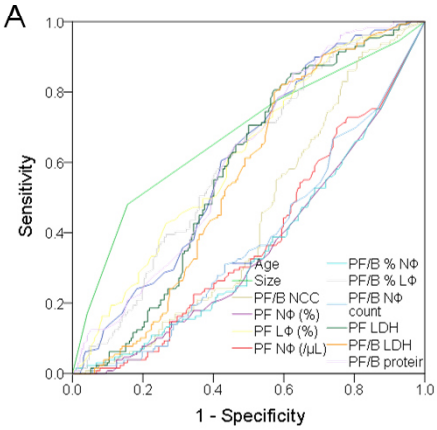

B

Variable	AUC	*P*	95% CI	Cut-off
Age (years)	0.600	0.014	0.524-0.676	> 55
PE size (score 1-5)	0.719	10^{-7}	0.646-0.791	> 3
PF/B NCC ratio	0.418	0.046	0.341-0.495	< 0.05
PF NΦ (%)	0.347	2×10^{-4}	0.272-0.421	< 10
PF LΦ (%)	0.617	0.004	0.539-0.694	> 40
PF NΦ (/μL)	0.361	6×10^{-4}	0.286-0.436	< 60
PF/B NΦ % ratio	0.343	10^{-4}	0.269-0.417	< 0.1
PF/B LΦ % ratio	0.592	0.024	0.514-0.670	> 1.4
PF/B NΦ count ratio	0.361	7×10^{-4}	0.287-0.436	< 0.1
PF LDH (U/L)	0.622	0.003	0.546-0.697	> 250
PF/B LDH ratio	0.592	0.025	0.516-0.667	> 0.9
PF/B protein ratio	0.600	0.003	0.545-0.694	> 0.6

C

Variable	*P*	RR	95% CI
Age	10^{-6}	1.056	1.033-1.079
PE size	3×10^{-9}	2.817	2.002-3.965
PF NΦ (%)	8×10^{-4}	0.977	0.964-0.990
PF protein	10^{-4}	1.578	1.211-2.056
PE side	0.0299	3.779	1.138-12.544

D

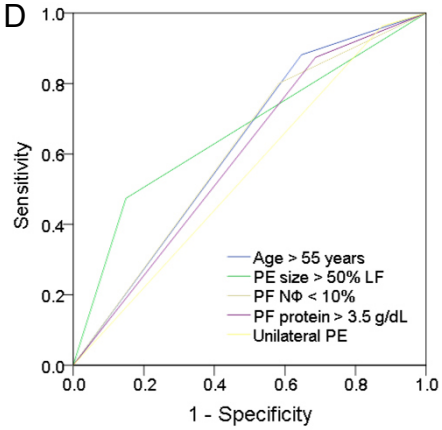

E

Variable	AUC	*P*	95% CI
Age > 55 years	0.617	3×10^{-4}	0.558-0.677
PE size > 50% LF	0.662	5×10^{-7}	0.601-0.724
PF NΦ < 10%	0.609	7×10^{-4}	0.548-0.669
PF protein > 3.5 g/dL	0.594	4×10^{-3}	0.533-0.654
Unilateral PE	0.544	0.045	0.502-0.599

F

Variable	*P*	RR	95% CI	**Risk points**
Age > 55 years	3×10^{-8}	8.130	3.873-17.065	**2**
PE size score > 3	1×10^{-10}	8.571	4.467-16.444	**2**
PF NΦ < 10%	1×10^{-4}	3.328	1.812-6.110	**1**
PF protein > 3.5 g/dL	2×10^{-4}	3.771	1.857-7.657	**1**
Unilateral PE	0.041	3.339	1.051-10.612	**1**

Figure 5.The MAPED score and its components. (A) Schematic representation of the components and relative weight of the variables that comprise MAPED. **(B) Heatmap of raw data used to compile the MAPED score.** ID, identification number; PE, pleural effusion; PF, pleural fluid.

Figure 5

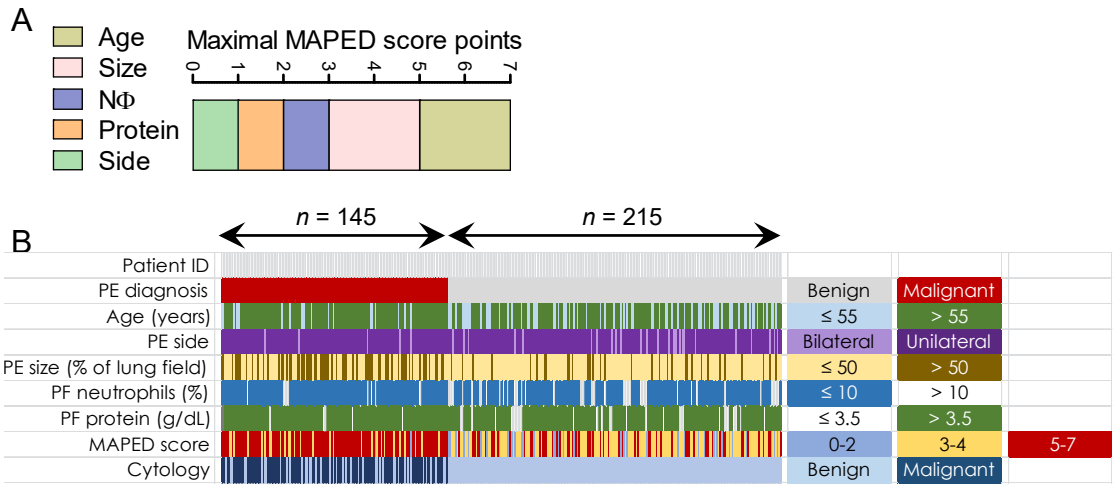
A
Age
Size
NΦ
Protein
Side
Maximal MAPED score points
0
1
2
3
4
5
6
7
B
n = 145
n = 215
Patient ID
PE diagnosis
Age (years)
PE side
PE size (% of lung field)
PF neutrophils (%)
PF protein (g/dL)
MAPED score
Cytology
Benign
Malignant
≤ 55
> 55
Bilateral
Unilateral
≤ 50
> 50
≤ 10
> 10
≤ 3.5
> 3.5
0-2
3-4
5-7
Benign
Malignant

Figure 6. Performance of the MAPED score in the discovery cohort. (A) Crosstabulation of MAPED score values by PE diagnosis. Shown are patient numbers (*n*) and percentages with Fischer's exact probability (*P*). Colors indicate frequencies by diagnosis. **(B)** Receiver-operator curve of MAPED targeting MPE diagnosis with area under curve (AUC), 95% confidence interval (95% CI), probability (*P*), and sensitivity and specificity values for two different MAPED cut-offs. **(C)** MAPED score patient distribution pie charts by diagnosis. **(D)** Probability of MPE by MAPED score. **(E)** MAPED score patient distribution violin plot by cytology result. *P*, probability for comparison of BPE-MPE distribution by Kolmogorov-Smirnov test. **(F)** MAPED score patient distribution violin plot by final diagnosis. *P*, probability for comparison of BPE-MPE distribution by Kolmogorov-Smirnov test. Colored dashed lines indicate cut-offs corresponding to Figure 6B. **(G)** Receiver-operator curve of MAPED targeting cytology results with area under curve (AUC), 95% confidence interval (95% CI), and probability (*P*). *n*, sample size; MAPED, malignancy of pleural effusion determined in the emergency department score.

Figure 6

A

$P = 4 \times 10^{-21}$	MAPED score							
n(%)	**0**	**1**	**2**	**3**	**4**	**5**	**6**	**7**
Benign	2(1)	8(4)	29(14)	50(23)	67(31)	49(23)	4(2)	6(3)
Malignant	0(0)	0(0)	2(1)	6(4)	22(15)	63(43)	22(15)	30(21)

0-10%
10-20%
20-30%
30-40%
40-50%
Frequency

B

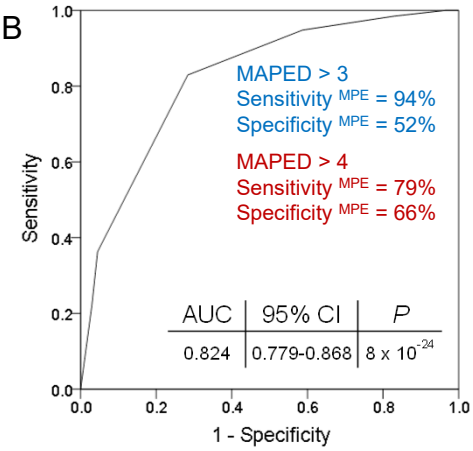

C

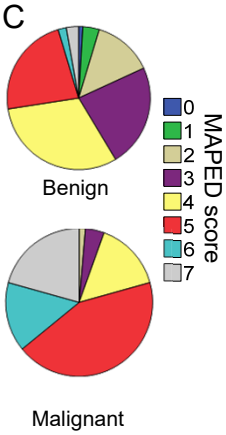

D

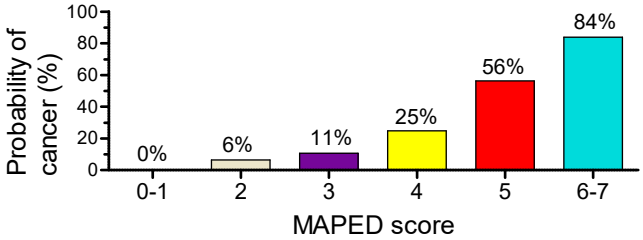

E

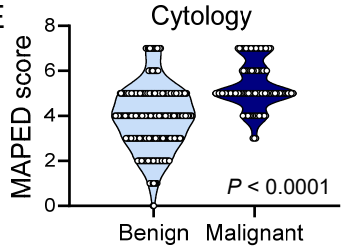

F

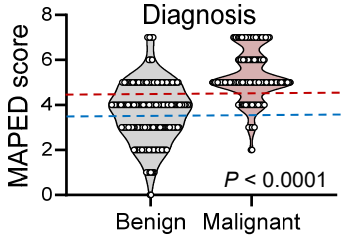

G

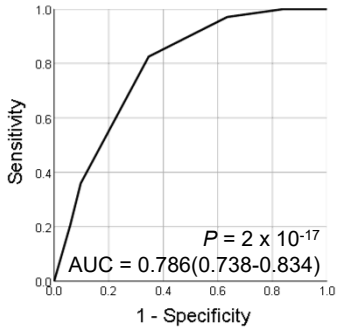

Figure 7. Comparison of the MAPED score with classical and modified Light's criteria in the derivation cohort. (A,B) Crosstabulation of MAPED score values by classical (LC^{CLASS}; pleural fluid LDH > 230 U/L, pleural fluid/serum LDH ratio > 0.6, or pleural fluid/serum protein ratio > 0.5) and modified (LC^{MOD}; pleural fluid LDH > 250 U/L, pleural fluid/serum LDH ratio > 0.9, or pleural fluid/serum protein ratio > 0.6) Light's criteria. Shown are patient numbers (*n*) and percentages with Fischer's exact probabilities (*P*) and kappa measures of agreement (κ). Colors indicate frequencies by no or any Light's criterion present. **(C)** Heatmap of associations between MAPED score, Light's criteria, and MPE diagnosis. Shown are color-coded Fischer's exact probabilities (*P*) from crosstabulations. **(D)** Receiver-operator curves (ROC) of MAPED and Light's criteria targeting MPE diagnosis with areas under curve (AUC), 95% confidence intervals (95% CI), and probabilities (*P*). *n*, sample size; MAPED, malignancy of pleural effusion determined in the emergency department score.

Figure 7

A

P = 0.003	MAPED score								0-10
n(%)	**0**	**1**	**2**	**3**	**4**	**5**	**6**	**7**	10-20
No LC^{CLASS}	0(0)	0(0)	6(21)	10(35)	9(31)	4(14)	0(0)	0(0)	20-30
≥ 1 LC^{CLASS}	2(1)	6(2)	25(8)	46(14)	80(25)	107(33)	22(7)	36(11)	30-40

κ = 0.001

Frequency (%)

B

P = 0.022	MAPED score								0-10
n(%)	**0**	**1**	**2**	**3**	**4**	**5**	**6**	**7**	10-20
No LC^{MOD}	0(0)	1(2)	8(16)	13(26)	15(30)	7(14)	4(8)	2(4)	20-30
≥ 1 LC^{MOD}	2(1)	7(2)	23(7)	43(14)	74(24)	105(34)	22(7)	34(11)	30-40

κ = -0.0005

Frequency (%)

C

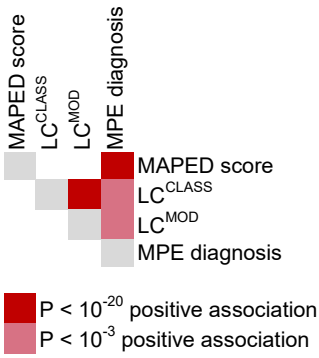

D

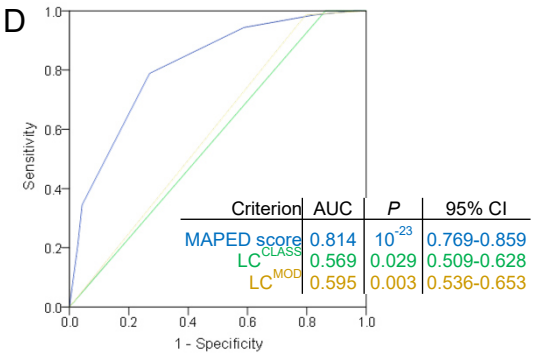

Figure 8. Performance of the MAPED score in the Oxford validation cohort. (A) Crosstabulation of MAPED score values by PE diagnosis. Shown are patient numbers (*n*) and percentages with Fischer's exact probability (*P*). Colors indicate frequencies by diagnosis.**(B)** Receiver-operator curve of MAPED targeting MPE diagnosis with area under curve (AUC), 95% confidence interval (95% CI), probability (*P*), and sensitivity and specificity values for two different MAPED cut-offs. **(C)** MAPED score patient distribution pie charts by diagnosis. **(D)** Probability of MPE by MAPED score, including probabilities of no difference by two-way ANOVA for comparison of MPE likelihoods by MAPED score in the Patras derivation and Oxford validation cohorts. P^{MAPED}, probability of no difference by MAPED score and P^{SITE}, probability of no difference by study site. *n*, sample size; MAPED, malignancy of pleural effusion determined in the emergency department score.

Figure 8

A

P = 0.0001	MAPED score							0-10%
n(%)	**1**	**2**	**3**	**4**	**5**	**6**	**7**	10-20%
Benign	3(2)	7(5)	27(21)	43(34)	26(20)	13(10)	9(7)	20-30%
Malignant	1(1)	1(1)	10(9)	23(20)	37(33)	28(25)	13(12)	30-40%

Frequency

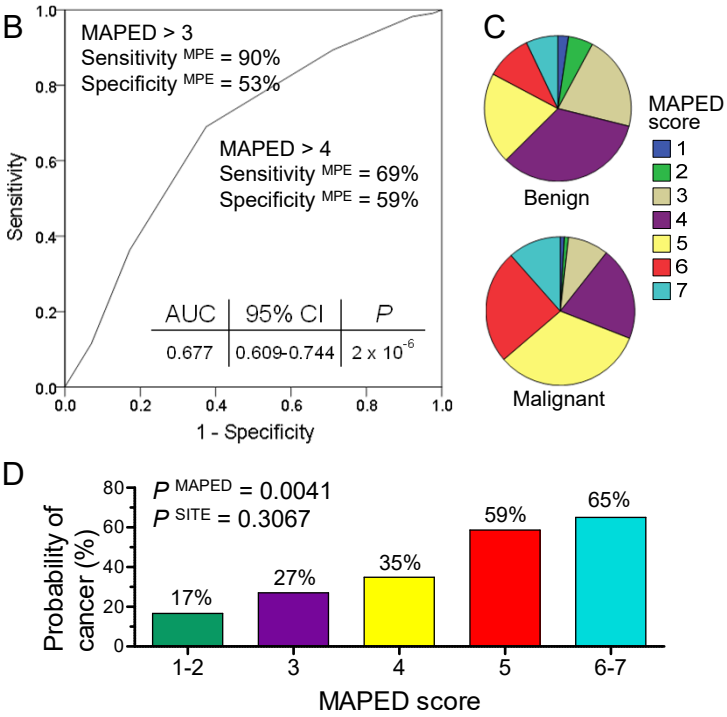

Figure 9. Cross-examination of MAPED with computationally-identified MAPED clusters. (A) Unsupervised hierarchical clustering of the MAPED cohort (*n* = 360) using ConsensusCluster (6), identifies two major patient groups defined by pleural effusion size and protein content on binary logistic regression. Shown are color-coded pivot tables of ConsensusCluster, MAPED score, and outcome data sorted automatically by ConsensusCluster **(A)** or MAPED score **(B)**. Columns represent individual patients and rows variables entered. Shown are Fischer'sexact test probabilities (*P*) from crosstabulations of ConsensusCluster **(A)** or MAPED score **(B)** by diagnosis. *n*, sample size; PE, pleural effusion; PF, pleural fluid; LF, lung field; MAPED, malignancy of pleural effusion determined in the emergency department score.

Figure 9

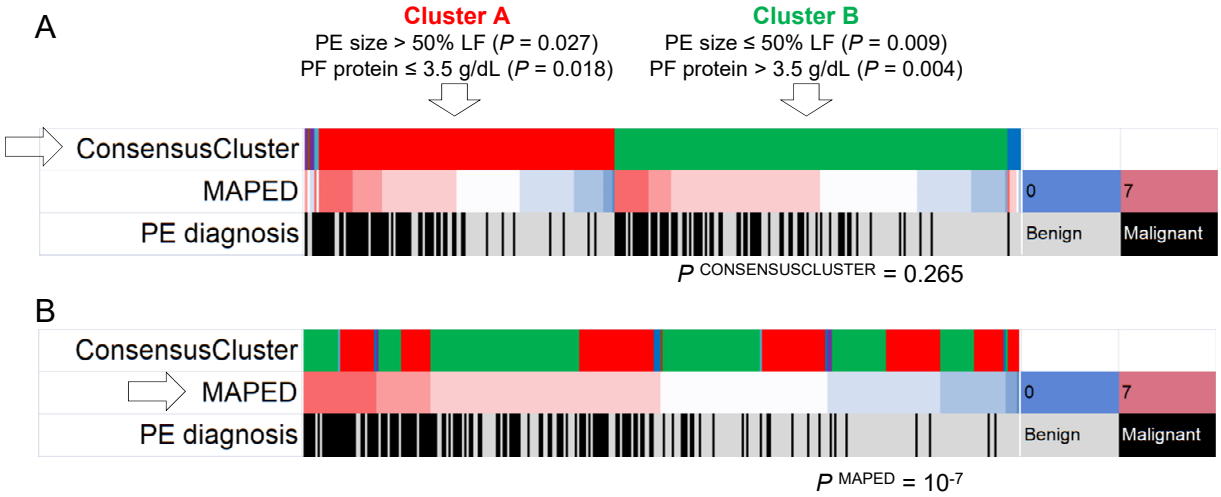
A
Cluster A
PE size > 50% LF (P = 0.027)
PF protein ≤ 3.5 g/dL (P = 0.018)
Cluster B
PE size ≤ 50% LF (P = 0.009)
PF protein > 3.5 g/dL (P = 0.004)
ConsensusCluster
MAPED
PE diagnosis
0
7
Benign
Malignant
P CONSENSUSCLUSTER = 0.265
B
ConsensusCluster
MAPED
PE diagnosis
0
7
Benign
Malignant
P MAPED = 10-7

TABLES

Table 1. Summary of MAPED patient data at entry by primary outcome.

Pleural effusion diagnosis	**Benign**	**Malignant**
n	215	145
Age [years; mean(95%CI)]* **	61(59–64)	68(67–70)
Sex (female/male)	105/110	66/79
Smoking (never/former/current)	70/51/94	42/37/66
Pleural effusion side (right/left/bilateral)*	111/77/27	86/54/5
Pleural effusion size score (0-10/11-25/26-50/51-75/76-100 % of lung field)* **	16/75/90/22/12	7/22/49/44/23
Fulfilment of Light's criteria of exudate (no/yes)§	29/182	0/142

* and ***: $P < 0.05$ and $P < 0.001$, respectively, by Mann Whitney test or χ^2 test, as appropriate.

§: Note that 4 benign and 3 malignant PE could not be characterized according to Light because of missing data.

MAPED, malignancy of pleural effusion determined in the emergency department score.

Table 2. MAPED score elements and score for each category.

MAPED elements	**Risk points**
Age> 55 years	2
Pleural Effusion Size> 50% of lung field	2
Pleural Neutrophil percentage<10%	1
Protein> 3.5 g/dL	1
Unilateral Pleural Effusion	1

MAPED, malignancy of pleural effusion determined in the emergency department score.